

## Original Full Length Article

# Mechanotransduction in bone tissue: The A214V and G171V mutations in Lrp5 enhance load-induced osteogenesis in a surface-selective manner<sup>☆</sup>

Paul J. Niziolek<sup>a,b</sup>, Matthew L. Warman<sup>c,d</sup>, Alexander G. Robling<sup>a,e,\*</sup>

<sup>a</sup> Department of Anatomy & Cell Biology, Indiana University School of Medicine, Indianapolis, IN, USA

<sup>b</sup> Weldon School of Biomedical Engineering, Purdue University, West Lafayette, IN, USA

<sup>c</sup> Department of Orthopaedic Surgery, Children's Hospital, Boston, MA, USA

<sup>d</sup> Howard Hughes Medical Institute, Department of Genetics, Harvard Medical School, Boston, MA, USA

<sup>e</sup> Department of Biomedical Engineering, Indiana University-Purdue University at Indianapolis (IUPUI), Indianapolis, IN, USA

## ARTICLE INFO

## Article history:

Received 21 March 2012

Revised 8 May 2012

Accepted 25 May 2012

Available online xxx

Edited by: Robert Recker

## Keywords:

Wnt

Lrp5

HBM

Loading

Mechanotransduction

Osteoporosis

## ABSTRACT

Mechanotransduction in bone requires components of the Wnt signaling pathway to produce structurally adapted bone elements. In particular, the Wnt co-receptor LDL-receptor-related protein 5 (LRP5) appears to be a crucial protein in the mechanotransduction cascades that translate physical tissue deformation into new bone formation. Recently discovered missense mutations in LRP5 are associated with high bone mass (HBM), and the altered function of these proteins provide insight into LRP5 function in many skeletal processes, including mechanotransduction. We further investigated the role of LRP5 in bone cell mechanotransduction by applying mechanical stimulation *in vivo* to two different mutant mouse lines, which harbor HBM-causing missense mutations in Lrp5. Axial tibia loading was applied to mature male Lrp5 G171V and Lrp5 A214V knock-in mice, and to their wild type controls. Fluorochrome labeling revealed that 3 days of loading resulted in a significantly enhanced periosteal response in the A214V knock in mice, whereas the G171V mice exhibited a lowered osteogenic threshold on the endocortical surface. In summary, our data further highlight the importance of Lrp5 in bone cell mechanotransduction, and indicate that the HBM-causing mutations in Lrp5 can alter the anabolic response to mechanical stimulation in favor of increased bone gain.

© 2012 Published by Elsevier Inc.

## Introduction

Mechanical loading of bone induces adaptive changes in the bone structure and geometry, achieved by altered bone resorption and formation activity [1,2]. *In vivo* experiments in rodents show that exogenous mechanical loading of bone tissue leads to increased transcription of WNT/ $\beta$ -catenin responsive genes and reporter molecules in osteocytes, and that unloading of bone leads to decreased WNT/ $\beta$ -catenin signaling due to increased sclerostin expression [3–5]. These results have been confirmed *in vitro*, where cultured bone cells express WNT/ $\beta$ -catenin responsive genes in response to mechanical stimulation [4,6]. An important component of the WNT/ $\beta$ -catenin signaling pathway in bone is the low density lipoprotein receptor-related protein 5 (LRP5), a WNT co-receptor that plays a major role in bone mass regulation in humans and mice [7–11].

Beyond its general role in bone metabolism, LRP5 is necessary for load induced bone formation. We previously reported that Lrp5 knock-out mice have an almost complete ablation of the anabolic response to mechanical loading of the ulna, compared to wild-type (WT) relatives [12]. These effects have been confirmed in another, independently generated Lrp5 knockout mouse, using a different loading model [13]. Moreover, clinical data also support the role of LRP5 signaling in regulating bone mechanotransduction. In a large human sample, Kiel et al. reported that several single nucleotide polymorphisms (SNPs) in LRP5, located in exons 10 and 18, significantly affected the relation between physical activity and bone mass accrual [14]. Collectively, these observations indicate that LRP5 is a critical component of the mechanical signaling cascade in bone.

Certain missense mutations near the N-terminus of LRP5 have been reported to cause a high bone mass (HBM) phenotype in humans [8,9,15,16]. *In vitro* experiments in cell lines transfected with LRP5 HBM mutations revealed that the mutation confers resistance to the endogenous Lrp5 antagonists, Dkk1 [8,17,18] and sclerostin [19–23]. The observed resistance to these and other Lrp5 inhibitors might be the mechanism by which the HBM phenotype emerges in humans and mice.

<sup>☆</sup> This work was supported by NIH grant AR53237 (to AGR), and by the Howard Hughes Medical Institute (to MLW).

\* Corresponding author at: Department of Anatomy & Cell Biology, Indiana University School of Medicine, 635 Barnhill Dr., MS 5035, Indianapolis, IN 46202, USA. Fax: +1 317 278 2040.

E-mail address: [arobling@iupui.edu](mailto:arobling@iupui.edu) (A.G. Robling).

Several years ago, a mouse model for the LRP5 HBM phenotype was generated using a transgenic overexpression approach. Those mice harbor a transgene coding for the human LRP5 G171V HBM mutation, driven by a 3.6 kb fragment of the rat *Collα1* promoter [7]. This mouse strain exhibits significantly increased bone mineral density, similar to that seen in humans. Overall, the mice have higher bone structural strength (ultimate force, yield force, and stiffness) and apparent material properties (ultimate stress, yield stress, and flexural modulus) [24]. This mouse was also reported to have an increased sensitivity to load, due to a lower threshold for initiating bone formation [4,13]. More recently, we reported the development of two Lrp5 HBM mouse models, in which we have knocked-in the G171V or A214V missense mutations into the endogenous *Lrp5* sequence [25,26]. These mice express the HBM mutant receptors at normal levels and in normal (naturally occurring) tissues, due to retention of the endogenous *Lrp5* promoter driving transcription. Similar to the HBM patients, we have found that both knock-in mouse lines have a strong HBM phenotype.

The non-invasive rodent axial tibial-loading model has been developed to apply a controlled mechanical load to the tibia through the knee and ankle joints [27,28]. This model presents an alternative to the ulnar loading model, which directly applies a load to the ulna at the proximal end. Because the axial tibia loading model applies force to the tibia through the proximal and distal joint surfaces, the loading environment might more closely approximate the physiological application of load.

In the present communication, we investigated the cortical bone formation response in *Lrp5* G171V and A214V knock-in and wild-type (WT) mice, after application of an equivalent mechanical stimulus using the non-invasive tibial-loading model. We hypothesized that both HBM-causing mutations would result in larger load-induced bone formation parameters compared to the WT mice. We found that A214V mice had significantly greater periosteal bone formation compared to WT at the proximal and midshaft locations of the tibia. However, periosteal bone formation at all sites in G171V mice was not significantly greater than was observed in WT mice. On the endocortical surface, we observed a significant load-induced upregulation of bone formation only in the G171V mice, indicating that G171V mice may have a lower strain threshold for bone formation. In summary, our data further highlight the importance of *Lrp5* in bone cell mechanotransduction, and indicate that the HBM-

causing mutations in *Lrp5* can alter the anabolic response to mechanical stimulation in favor of increased bone gain.

## Materials and methods

### Animals

Generation of knock-in mice with the A214V and G171V mutations in *Lrp5* has been described previously [25]. Briefly, two targeting constructs spanning introns 2–4 were generated, which harbored the G171V or A214V mutation located in exon 3. The constructs were introduced into mouse embryonic stem (ES) cells, and standard selection techniques were used to identify clones in which the construct properly recombined into the endogenous *Lrp5* sequence. The ES cells were implanted into pseudopregnant females, and chimeric pups were identified and bred using standard techniques. The mice were bred to homozygosity (*Lrp5*<sup>+/+</sup> [designated as WT], *Lrp5*<sup>A214V/A214V</sup> [designated as *Lrp5* A214V], or *Lrp5*<sup>G171V/G171V</sup> [designated as *Lrp5* G171V]). The genetic background of all mice was a uniform mixture of 129S1/SvIMJ and C57Bl/6J. All animal procedures performed in accordance with guidelines set by the Indiana University Institutional Animal Care and Use Committee.

### Strain gage measurements

Four 18 week-old male mice homozygous for one of the three *Lrp5* genotypes (WT, A214V, G171V) were sacrificed and right hindlimb was frozen at  $-20^{\circ}\text{C}$  until strain gage testing. Limbs were allowed to warm to room temperature over several hours and muscle tissue was carefully dissected away to reveal the midshaft tibia. A strain gage (EA-06-015DJ-120, Vishay) was applied to midshaft of tibia on the posterior surface (surface between tibia and fibula) and the tibia was placed into the loading cups (Figs. 1A and B). We determined the microstrain:load ratio for each sample using progressively increasing load applications while simultaneously recording the voltage output from the load cell and strain gage. All tests were averaged within each genotype to determine the microstrain:load ratio for each genotype. A peak microstrain value of 2120 was chosen to be applied to all genotypes and this corresponded to peak loads of 9.0, 14.4, and 9.8 N for WT, A214V, G171V genotypes, respectively (Fig. 1A).

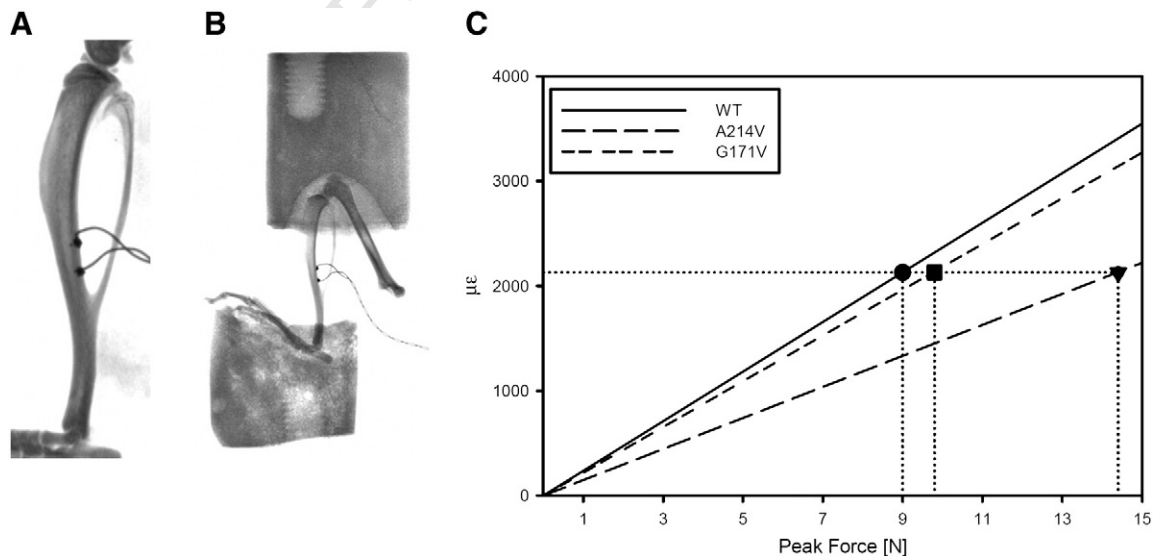


**Fig. 1.** A) X-ray of excised tibia with strain gage attached at the posterior midshaft (surface between tibia and fibula). Gages were placed on 4 specimens for each *Lrp5* genotype (WT, A214V, G171V) and each specimen was tested 1–4 times to determine the microstrain ( $\mu\epsilon$ ) to compressive force ratio. B) X-ray of excised lower limb in loading cups. C) The  $\mu\epsilon$ :force ratio for the tibial midshaft as determined from strain gage testing. A peak value of 2120  $\mu\epsilon$  was chosen to apply to the three genotypes in the tibia loading experiment. This peak strain corresponded to a peak force of 9.0 N, 9.8 N, and 14.4 N in the WT, G171V, and A214V mice, respectively.

## 160 Loading protocol

161 At 18 weeks of age, 8 male mice of each *Lrp5* genotype (WT,  
162 A214V, G171V) began the axial tibia loading protocol. Mice were  
163 anesthetized using isoflurane inhalation, and their right hindlimb  
164 (knee to foot) was placed in molded loading cups that secured the  
165 tibia (Fig. 1B). A sinusoidal wave form (2 Hz, 120 cycles) was applied  
166 with a peak load as described above. Mice were given three bouts  
167 with a day of rest between each bout. Intraperitoneal injection of alizarin  
168 was given 1 day after the final bout followed by an intraperitoneal  
169 injection of calcein 8 days later. Mice were sacrificed 17 days after  
170 the final bout. The right and left tibias were harvested and placed in  
171 10% NBF for 2 days followed by storage in 70% ethanol at 4 °C.

## 172 Histological processing and measurements

173 Tibias were dehydrated in graded alcohols, cleared in xylene, and  
174 embedded in methylmethacrylate following standard protocols.  
175 Thick-cut sections were taken at locations 25% (proximal), 50%  
176 (midshaft), and 75% (distal) of total tibia length and ground down  
177 to ~30 µm. A single unstained section from each tibia was digitally  
178 imaged on a fluorescent microscope using filter sets that provide  
179 excitation and emission for the calcein and alizarin wavelengths  
180 (Fig. 2). Digital images were imported into ImagePro Express  
181 (Media Cybernetics, Inc., Gaithersburg, MD) and the following  
182 histomorphometric measurements were recorded for the endosteal  
183 and periosteal surfaces: total perimeter, single label perimeter  
184 (sLPm), double label area and perimeter, total bone area and marrow  
185 area. The following results were calculated: double label perimeter  
186 (dLPm = double label circumference/2), mineral apposition rate  
187 (MAR = double label area/dLPm/8 days), mineralizing surface (MS/  
188 BS = (0.5 × sLPm + dLPm)/total perimeter × 100), and bone forma-  
189 tion rate (BFR/BS = MAR × MS/BS × 3.65)

## 190 Statistical methods

191 Measurements comparing right (loaded) vs left (non-loaded)  
192 bones were analyzed for statistical significance using a paired stu-  
193 dent's *t*-test. Measurements comparing genotypes used relative  
194 values, calculated by subtracting the nonloaded (left leg) values

from the loaded (right leg) values, to account for differences within  
195 a mouse. Student's *t*-test was used to compare *Lrp5* HBM mice to  
196 WT mice. Significance was taken at  $p < 0.05$ .  
197

## 198 Results

199 Control limb bone formation parameters are similar among *Lrp5* WT,  
200 A214V, and G171V mice at 20 wks of age

201 To assess baseline bone formation rates among the three *Lrp5* ge-  
202 notypes, left (nonloaded) tibial bone formation parameters were  
203 measured and compared. Mineral apposition rates (MAR), mineraliz-  
204 ing surface (MS/BS), and bone formation rates (BFR/BS) were similar  
205 among all three genotypes, for both endocortical and periosteal sur-  
206 faces and at all three diaphyseal locations, with one exception  
207 (Table 1). The only parameter that was significantly affected by geno-  
208 type was periosteal MS/BS at the proximal diaphyseal location. Post-  
209 hoc tests revealed that the *Lrp5* G214V mice had significantly reduced  
210 ( $p = 0.02$ ) proximal tibia periosteal MS/BS, compared to WT mice.

211 Mechanical loading increases periosteal bone formation in the tibia, and  
212 *Lrp5* A214V mice have an increased load-induced periosteal bone  
213 formation response compared to WT mice

214 The axial tibia loading model induced a significant increase in peri-  
215 osteal bone formation in the loaded limb compared to non-loaded  
216 limb in all three genotypes examined (Table 1). However, this effect  
217 was observed only for the proximal and midshaft locations, but not  
218 at the distal location (with the exception of increased periosteal  
219 MAR in the A214V mice). Comparison of the loading response in  
220 HBM mice to that measured for WT mice was facilitated by calculating  
221 relative (*r*) bone formation parameters for each mouse; i.e., sub-  
222 tracting the loaded (right) limb parameters from the corresponding  
223 non-loaded (left) limb to account for baseline differences within an  
224 animal. Compared to WT mice, A214V mice had significantly increased  
225 MAR, MS/BS, and BFR/BS at the proximal site, and significantly in-  
226 creased MAR and BFR/BS at the midshaft, but no significant differences  
227 from WT at the distal site (Fig. 3). Relative periosteal bone formation  
228 parameters among the G171V mice were not significantly different  
229 from those measured in the WT mice, at all three diaphyseal locations.

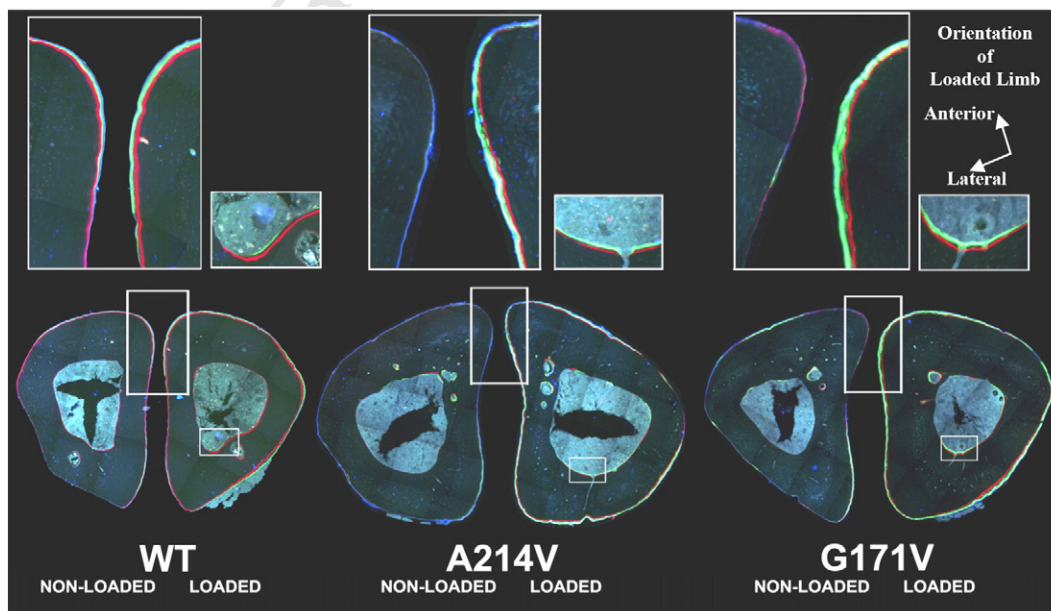


Fig. 2. Mosaic images of non-loaded (left) and loaded (right) midshaft tibias for WT, A214V, and G171V mice. Upper panels magnify (300%) the respective areas highlighted below them (left: periosteal surface; right: endosteal surface).

**Table 1**  
Summary of tibial dynamic histomorphometric parameters from right and left limbs, at periosteal and endocortical surfaces, and at three diaphyseal locations.

Region			
Surface			
Lrp5 genotype	MAR ( $\mu\text{m}/\text{day}$ )	MS/BS (%)	BFR/BS ( $\mu\text{m}^3/\mu\text{m}^2/\text{yr}$ )
Side			
Proximal location			
Periosteal surface			
WT			
Right (loaded)	0.30 ± 0.06	80 ± 11	94 ± 22
Left (control)	0.62 ± 0.07*	143 ± 21*	349 ± 86*
A214V			
Right (loaded)	0.35 ± 0.03	67 ± 14	88 ± 23
Left (control)	0.91 ± 0.05*	192 ± 9*	646 ± 54*
G171V			
Right (loaded)	0.26 ± 0.07	36 ± 7	43 ± 13
Left (control)	0.70 ± 0.05*	143 ± 18*	381 ± 69*
Midshaft location			
Periosteal surface			
WT			
Right (loaded)	0.29 ± 0.04	50 ± 7	57 ± 14
Left (control)	0.48 ± 0.05*	79 ± 7*	146 ± 23*
A214V			
Right (loaded)	0.21 ± 0.04	45 ± 9	42 ± 16
Left (control)	0.59 ± 0.05*	88 ± 3*	192 ± 20*
G171V			
Right (loaded)	0.23 ± 0.05	35 ± 6	32 ± 6
Left (control)	0.51 ± 0.06*	77 ± 5*	151 ± 27*
Endocortical surface			
WT			
Right (loaded)	0.36 ± 0.05	36 ± 10	50 ± 17
Left (control)	0.44 ± 0.07	49 ± 7	90 ± 23
A214V			
Right (loaded)	0.35 ± 0.07	29 ± 5	40 ± 9
Left (control)	0.45 ± 0.05	32 ± 5	52 ± 10
G171V			
Right (loaded)	0.27 ± 0.06	28 ± 4	30 ± 11
Left (control)	0.45 ± 0.04*	48 ± 6*	83 ± 15*
Distal location			
Periosteal surface			
WT			
Right (loaded)	0.16 ± 0.06	43 ± 8	35 ± 17
Left (control)	0.22 ± 0.05	42 ± 7	40 ± 14
A214V			
Right (loaded)	0.19 ± 0.06	34 ± 13	43 ± 23
Left (control)	0.26 ± 0.06*	47 ± 9	56 ± 19
G171V			
Right (loaded)	0.08 ± 0.03	13 ± 5	7 ± 4
Left (control)	0.18 ± 0.06	25 ± 10	31 ± 1
Endocortical surface			
WT			
Right (loaded)	0.37 ± 0.03	38 ± 5	54 ± 9
Left (control)	0.46 ± 0.04	36 ± 4	61 ± 9
A214V			
Right (loaded)	0.28 ± 0.07	47 ± 5	53 ± 15
Left (control)	0.37 ± 0.08	43 ± 9	73 ± 20
G171V			
Right (loaded)	0.16 ± 0.08	31 ± 15	48 ± 29
Left (control)	0.26 ± 0.07	41 ± 11	57 ± 23

Mean ± standard error are reported.

\* p < 0.05 paired t-test nonloaded (left) vs loaded (right) limb.

#### Lrp5 G171V mice require less strain to activate load-induced endocortical bone formation

In WT mice, we were unable to detect a significant increase in bone formation parameters on the endocortical surface of the loaded tibiae compared to the same surface in the control tibiae. A similar lack of load-responsiveness was found on the endocortical surface of A214V tibiae. However, the loaded limbs from G171V mice had significantly increased endocortical bone formation parameters at the midshaft location compared to the non-loaded limb (Table 1). It is unclear

whether this effect existed at the proximal site in these mice as we were not able to reasonably measure the endosteal surface at the proximal location due to trabeculae disrupting the majority of the endosteal surface in the HBM mice. The increased load-induced bone formation rates on the endocortical surface of G171V mice, but not of WT mice, suggest that less strain was required to activate bone formation in these mice, i.e., a lower strain threshold for the endocortical surface appears to exist in the G171V mice.

#### Discussion

We investigated whether the Lrp5 HBM-causing missense mutations A214V and G171V, when expressed at naturally-occurring levels and in physiologically routine cell types, confer enhanced bone formation responsiveness to mechanical loading. Our broader goal was to shed some light on whether enhanced osteo-anabolic responsiveness to everyday loading events (e.g., locomotion, physical activity) might explain a portion of the mechanisms that induce the HBM phenotype. We found that while both HBM mutations improved mechanotransduction beyond the efficiency observed in WT mice, the A214V and G171V exerted their effects on this process differently. The A214V mutation, but not the G171V mutation, was associated with an enhanced response to mechanical loading on the periosteal surface, when compared to WT mice. On the endosteal surface, we observed that the G171V mutation, but not the A214V mutation or the WT allele, conferred increased bone formation in response to loading, suggesting that the strain threshold for endocortical bone formation was lowered by the G171V mutation.

Load induced bone formation was observed in two of the three locations along the tibial diaphysis. The distal site (75%) was not responsive to mechanical loading among any of the mouse genotypes, with the exception of periosteal MAR in the A214V mice. These findings suggest that the tibia axial loading model imposes an insufficient amount of strain to this site to reliably induce bone formation. Alternatively, the lack of bone curvature in the distal diaphysis, and the consequent lack of bending that would be expected from an axial load, might account for the non-responsiveness. In support of this explanation, the proximal site that we analyzed (25%) was equally distant from the closest joint surface as was the distal site, yet the curvature is much greater in the proximal end, and the proximal site responded robustly to the loading stimulus whereas the distal site did not. Others have also reported reduced or non-significant loading effects at the distal tibia using the tibia axial loading model [28,29].

We have previously shown that a reduction in sclerostin expression is temporally and spatially associated with mechanical strain magnitude, indicating that a loss of sclerostin-mediated Lrp5 suppression might play a role in the cellular signaling cascade that leads to load-induced bone formation [30]. This hypothesis is further strengthened by our recent ulnar loading experiments in <sup>8kb</sup>Dmp1::hSOST transgenic mice (an 8 kb fragment of the Dentin matrix protein 1 (Dmp1) promoter driving expression of human SOST), which exhibit a severe loss of mechanotransduction, similar to Lrp5 knock-out mice [31]. Presumably, these mice have increased expression/release of Lrp5 agonists (e.g., Wnt molecules), but the unrepressed transgenic expression of sclerostin prevents Wnt signaling through Lrp5. In vitro, it has been shown that several Lrp5 HBM mutations are resistant to Dkk1 and sclerostin binding [17,19,32]. Thus, if (1) HBM mutations confer immunity to sclerostin-mediated inhibition, and (2) loss of sclerostin is the sole determinant of whether mechanotransduction will occur, then we would expect to find equal bone formation in the loaded and non-loaded limbs of our HBM knock-in mice. In other words, the knock-in mice would be experiencing a constant mechanical loading signal in all bones, since they would not be inhibited by sclerostin (similar to removing sclerostin as a result of loading in WT mice). Because we observed

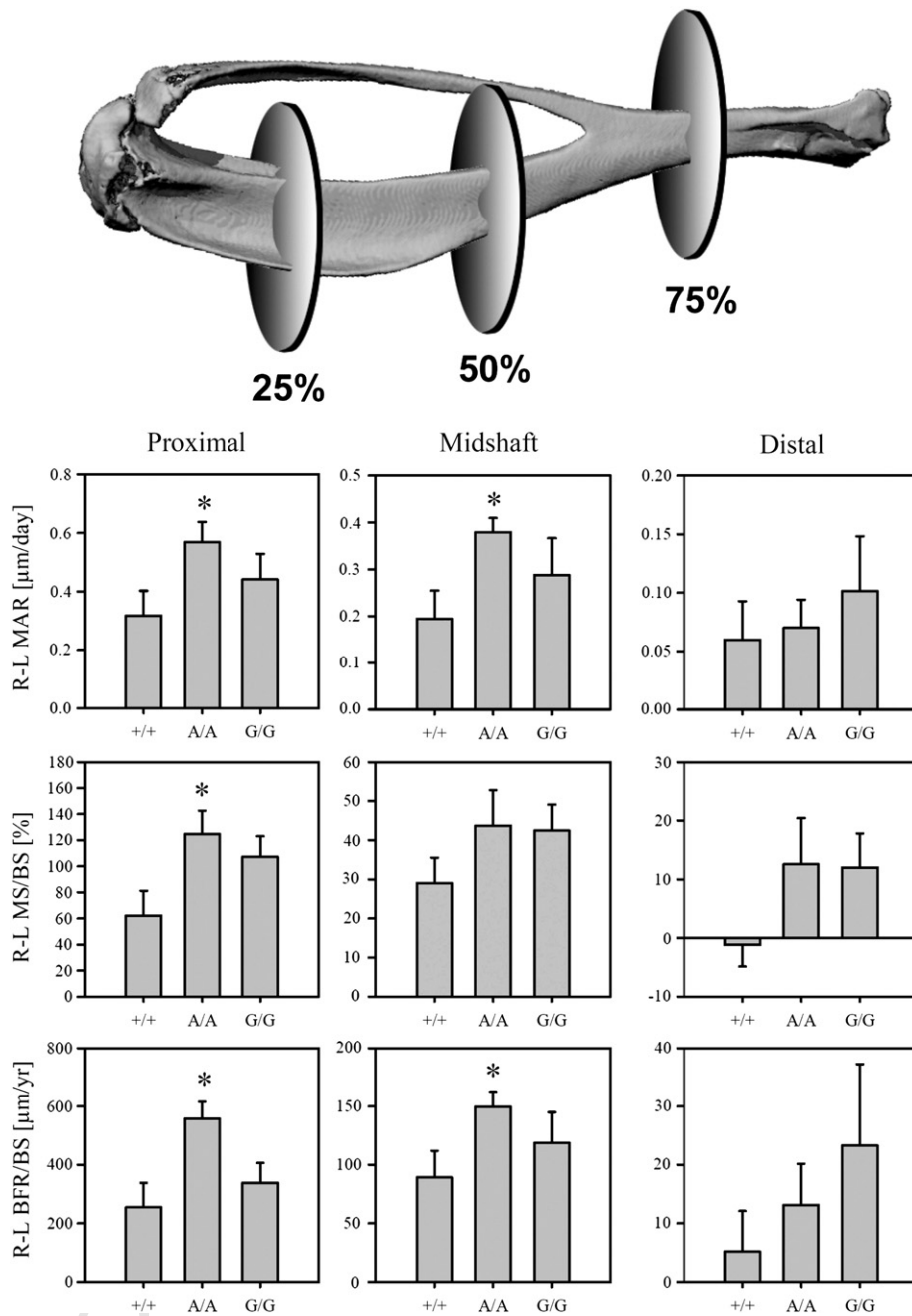


**Fig. 3.** On the periosteal surface, the Lrp5 A214V mutation conferred enhanced bone formation compared to WT mice. R-L (loaded–non-loaded limb) bone formation parameters indicate that at the proximal location (25% of length along tibial axis) the A214V mutation conferred an enhanced response to mineral apposition rate (MAR), mineralizing surface (MS/BS), and bone formation rate (BFR/BS) when compared to WT mice. At the midshaft, R-L MAR and R-L BFR/BS were both significantly enhanced by the A214V mutation. No differences in response were observed at the distal location (75% along tibial axis) nor for the G171V mutation at any periosteal location. \* =  $p < 0.05$  vs WT student's *t*-test,  $n = 7$ –8 per group.

303 load-induced bone gain in the knock-ins, our data indicate that  
 304 mechanotransduction through the Lrp5 receptor requires not only  
 305 the removal of Lrp5 inhibition, but also the upregulation/secretion  
 306 of ligand(s) for enhanced receptor activation, i.e., release of Wnts or  
 307 other Lrp5 agonists. Thus, the signaling mechanisms can be thought  
 308 of as a two-arm process: reduction of Lrp5 inhibitors and enhance-  
 309 ment of Lrp5 activators. If either arm is compromised, it is likely  
 310 that mechanotransduction will be compromised.

311 Published data on the Lrp5 G171V transgenic mouse (<sup>3.6kb</sup>Coll $\alpha$ 1::  
 312 G171V) report an enhancement in mechanical loading responsiveness  
 313 through a lowered threshold for bone formation [24,33]. Our Lrp5  
 314 G171V knock-in mice had a significant load-induced response on the

315 endocortical surface, but the same amount of mechanical strain applied  
 316 to WT mice did not elicit an endocortical response. Thus, our results  
 317 support the previously advanced hypothesis that the Lrp5 G171V muta-  
 318 tion lowers the mechanical strain threshold for bone formation. Fur-  
 319 thermore, we have reported that our two Lrp5 HBM mutant mice  
 320 have a different phenotype from one another, with G171V mice prefer-  
 321 entially adding more bone endosteally to result in a smaller medullary  
 322 area than WT mice, and the A214V preferentially adding more bone  
 323 periosteally to result in a larger total cross section than WT mice [26].  
 324 In that study, we observed no difference in non-loaded limb marrow  
 325 area in G171V compared to WT, but A214V had an increased marrow  
 326 area compared to wild type. Given the thicker cortices and smaller

marrow space of the G171V mice, we calculated the strains on the endocortical surface to be ~15% lower than those calculated for WT mice (data not shown). Despite these lower strains, the G171V mice were responsive to tibial loading, whereas WT mice were not.

On the periosteal surface, we did not observe an enhanced bone formation response in the G171V compared to WT mice, which differs from Akhter et al.'s report of an enhanced periosteal formation surface response per unit strain for the G171V transgenic mice [24]. This difference might be due to their use of two different values of peak strain; the same peak load was applied to both genotypes, instead of using different loads to apply the same peak strain as we did in this experiment [33]. Moreover, the loading models employed were different; we used the axial tibial model, which produces axial compression and bending, whereas Akhter et al. used the 4-point bending model, which produces a nearly pure bending moment in the tibial midshaft. A more likely explanation, however, is the difference in receptor expression between the two models. The <sup>3.6kb</sup>Collα1::G171V mouse has much higher levels of receptor expression than WT mouse. In fact, overexpression of WT LRP5 (<sup>3.6kb</sup>Collα1::LRP5), at levels similar to those found in the high-expressing <sup>3.6kb</sup>Collα1::G171V line, resulted in significantly increased bone mass. Those data suggest that receptor number, independent of its mutation state, can bone mass significantly. However, the much more robust phenotype of the <sup>3.6kb</sup>Collα1::G171V transgenics indicates that the HBM mutation has a much more dramatic effect on bone mass than the WT allele. Nonetheless, it is unclear if the <sup>3.6kb</sup>Collα1::LRP5 mice would have enhanced responsiveness to loading. Secondly, the <sup>3.6kb</sup>Collα1 promoter fragment directs HBM overexpression to a specific population of cells, which might not normally express the receptor. This might explain their periosteal phenotype, whereas our G171V phenotype was largely endocortical. Further, the <sup>3.6kb</sup>Collα1::G171V mice overexpress the HBM gene with concurrent expression of endogenous Lrp5, both of which would be expected to be activated (perhaps differently) upon loading. Our HBM knock-in mice do not express any WT Lrp5 so they are not affected by this issue. A more recent publication using compressive axial loading of the tibia in the same G171V overexpresser mouse model as used by Akhter et al., reported that the <sup>3.6kb</sup>Collα1::G171V transgene significantly enhanced loading effects on the endocortical surface (as measured by load-induced change in medullary area) but not on the periosteal surface (as measured by load-induced change in total area) [13]. This surface-specific loading result for the G171V transgenic model is similar to that found in our G171V knock-in model. Interestingly, Saxon et al. found a sex-specific tibial loading effect for Lrp5 knockout mice, where the male Lrp5 knockouts showed no response to loading but the female knockouts were difficult to interpret [13]. One of the limitations of the present study is that we examined load-induced bone formation only in males; thus we are unable to address sex-specific effects of the knock-in alleles in mechanotransduction.

It should be noted that we also measured proximal tibia trabecular bone formation rates via fluorochrome histomorphometry (using the same pair of labels used for the cortical rates), and also static parameters of the proximal tibia trabecular meshwork (e.g., BV/TV, Tb.N) via μCT, but neither of these analyses produced a significant loading effect in the mice (data not shown). This observation is not unexpected since (1) our 3-day loading schedule was designed for histomorphometric detection of bone formation rate changes and not for more dramatic changes needed for detection by μCT, and (2) the labeling schedule employed was designed to capture the more slow-growing cortical bone, rather than the more rapidly accumulating trabecular bone in the proximal tibia.

In conclusion, we found that the bone formation response to mechanical loading was surface-specific, depending on the Lrp5 alleles present. For all Lrp5 genotypes, we found a significant increase in bone formation parameters between the loaded and non-loaded

limbs on the periosteal surface. However, the A214V mutation, but not G171V, was associated with an enhanced periosteal response to mechanical loading at the proximal and midshaft tibial locations, compared to WT. Conversely, only the G171V mice achieved a significant increase in bone formation on the endosteal surface at the midshaft, suggesting a lowered threshold for bone formation in these mice. These results support the pivotal role of Lrp5 in bone mechanotransduction, and suggest that although both mutations generate a high bone mass phenotype, there may be differences in the actual mechanism that governs their achievement of this HBM phenotype.

## References

- [1] Robling AG, Hinant FM, Burr DB, Turner CH. Improved bone structure and strength after long-term mechanical loading is greatest if loading is separated into short bouts. *J Bone Miner Res* 2002;17(8):1545–54.
- [2] Warden SJ, Turner CH. Mechanotransduction in the cortical bone is most efficient at loading frequencies of 5–10 Hz. *Bone* 2004;34(2):261–70.
- [3] Lin C, et al. Sclerostin mediates bone response to mechanical unloading through antagonizing Wnt/beta-catenin signaling. *J Bone Miner Res* 2009;24(10):1651–61.
- [4] Robinson JA, et al. Wnt/beta-catenin signaling is a normal physiological response to mechanical loading in bone. *J Biol Chem* 2006;281(42):31720–8.
- [5] Bonewald LF, Johnson ML. Osteocytes, mechanosensing and Wnt signaling. *Bone* 2008;42(4):606–15.
- [6] Hens JR, et al. TOPGAL mice show that the canonical Wnt signaling pathway is active during bone development and growth and is activated by mechanical loading in vitro. *J Bone Miner Res* 2005;20(7):1103–13.
- [7] Babij P, et al. High bone mass in mice expressing a mutant LRP5 gene. *J Bone Miner Res* 2003;18(6):960–74.
- [8] Boyden LM, et al. High bone density due to a mutation in LDL-receptor-related protein 5. *N Engl J Med* 2002;346(20):1513–21.
- [9] Little RD, et al. A mutation in the LDL receptor-related protein 5 gene results in the autosomal dominant high-bone-mass trait. *Am J Hum Genet* 2002;70(1):11–9.
- [10] Ai MR, Heeger S, Bartels CF, Schelling DK. Clinical and molecular findings in osteoporosis–pseudoglioma syndrome. *Am J Hum Genet* 2005;77(5):741–53.
- [11] Gong Y, et al. LDL receptor-related protein 5 (LRP5) affects bone accrual and eye development. *Cell* 2001;107(4):513–23.
- [12] Sawakami K, et al. The Wnt co-receptor LRP5 is essential for skeletal mechanotransduction but not for the anabolic bone response to parathyroid hormone treatment. *J Biol Chem* 2006;281(33):23698–711.
- [13] Saxon LK, Jackson BF, Sugiyama T, Lanyon LE, Price JS. Analysis of multiple bone responses to graded strains above functional levels, and to disuse, in mice in vivo show that the human Lrp5 G171V High Bone Mass mutation increases the osteogenic response to loading but that lack of Lrp5 activity reduces it. *Bone* 2011;49(2):184–93.
- [14] Kiel DP, et al. Genetic variation at the low-density lipoprotein receptor-related protein 5 (LRP5) locus modulates Wnt signaling and the relationship of physical activity with bone mineral density in men. *Bone* 2007;40(3):587–96.
- [15] Johnson ML, et al. Linkage of a gene causing high bone mass to human chromosome 11 (11q12–13). *Am J Hum Genet* 1997;60(6):1326–32.
- [16] Van Wesenbeeck L, et al. Six novel missense mutations in the LDL receptor-related protein 5 (LRP5) gene in different conditions with an increased bone density. *Am J Hum Genet* 2003;72(3):763–71.
- [17] Ai M, Holmen SL, Van Hul W, Williams BO, Warman ML. Reduced affinity to and inhibition by DKK1 form a common mechanism by which high bone mass-associated missense mutations in LRP5 affect canonical Wnt signaling. *Mol Cell Biol* 2005;25(12):4946–55.
- [18] Bhat BM, et al. Structure-based mutation analysis shows the importance of LRP5 beta-propeller 1 in modulating Dkk1-mediated inhibition of Wnt signaling. *Gene* 2007;391(1–2):103–12.
- [19] Balemans W, et al. The binding between sclerostin and LRP5 is altered by DKK1 and by high-bone mass LRP5 mutations. *Calcif Tissue Int* 2008;82(6):445–53.
- [20] Ellies DL, et al. Bone density ligand, Sclerostin, directly interacts with LRP5 but not LRP5G171V to modulate Wnt activity. *J Bone Miner Res* 2006;21(11):1738–49.
- [21] Li X, et al. Sclerostin binds to LRP5/6 and antagonizes canonical Wnt signaling. *J Biol Chem* 2005;280(20):19883–7.
- [22] Semenov M, Tamai K, He X. SOST is a ligand for LRP5/LRP6 and a Wnt signaling inhibitor. *J Biol Chem* 2005;280(29):26770–5.
- [23] Semenov MV, He X. LRP5 mutations linked to high bone mass diseases cause reduced LRP5 binding and inhibition by SOST. *J Biol Chem* 2006;281(50):38276–84.
- [24] Akhter MP, et al. Bone biomechanical properties in LRP5 mutant mice. *Bone* 2004;35(1):162–9.
- [25] Cui Y, et al. Lrp5 functions in bone to regulate bone mass. *Nat Med* 2011;17(6):684–91.
- [26] Niziolek PJ, et al. High-bone-mass-producing mutations in the Wnt signaling pathway result in distinct skeletal phenotypes. *Bone* 2011;49(5):1010–9.

- 472 [27] De Souza RL, et al. Non-invasive axial loading of mouse tibiae increases cortical 481  
473 bone formation and modifies trabecular organization: a new model to study cortical 482  
474 and cancellous compartments in a single loaded element. *Bone* 2005;37(6):810–8. 483
- 475 [28] Fritton JC, Myers ER, Wright TM, van der Meulen MC. Loading induces site-specific 484 Q8  
476 increases in mineral content assessed by microcomputed tomography of the 485  
477 mouse tibia. *Bone* 2005;36(6):1030–8. 486
- 478 [29] Fritton JC, Myers ER, Wright TM, van der Meulen MC. Bone mass is preserved and 487  
479 cancellous architecture altered due to cyclic loading of the mouse tibia after 488  
480 orchidectomy. *J Bone Miner Res* 2008;23(5):663–71. 489
- [30] Robling AG, et al. Mechanical stimulation of bone in vivo reduces osteocyte 481  
expression of Sost/sclerostin. *J Biol Chem* 2008;283(9):5866–75. 482
- [31] Tu X, et al. Sost downregulation and local Wnt signaling are required for the oste- 483  
ogenic response to mechanical loading. *Bone* 2011. 484
- [32] Balemans W, et al. Novel LRP5 missense mutation in a patient with a high bone 485  
mass phenotype results in decreased DKK1-mediated inhibition of Wnt signaling. 486  
*J Bone Miner Res* 2007;22(5):708–16. 487
- [33] Cullen DM, et al. Bone sensitivity to mechanical loads with the Lrp5 HBM muta- 488  
tion. *J Bone Miner Res* 2002;17:S332–S. 489

UNCORRECTED PROOF